HHS Public Access

Author manuscript

J Am Chem Soc. Author manuscript; available in PMC 2022 April 07.

Published in final edited form as:

J Am Chem Soc. 2021 April 07; 143(13): 5141–5149. doi:10.1021/jacs.1c00990.

DCAF11 supports targeted protein degradation by electrophilic proteolysis-targeting chimeras

Xiaoyu Zhang[1,*], **Lena M. Luukkonen**[2], **Christie L. Eissler**[2], **Vincent M. Crowley**[1], **Yu Yamashita**[1], **Michael A. Schafroth**[1], **Shota Kikuchi**[2], **David S. Weinstein**[2], **Kent T. Symons**[2], **Brian E. Nordin**[2], **Joe L. Rodriguez**[2], **Thomas G. Wucherpfennig**[1], **Ludwig Bauer**[1], **Melissa M. Dix**[1], **Dean Stamos**[2], **Todd M. Kinsella**[2], **Gabriel M. Simon**[2], **Kristen A. Baltgalvis**[2], **Benjamin F. Cravatt**[1,*]

[1]The Department of Chemistry and The Skaggs Institute for Chemical Biology, The Scripps Research Institute, 10550 N. Torrey Pines Road, La Jolla, CA 92307

[2]Vividion Therapeutics, 5820 Nancy Ridge Dr, San Diego, CA 92121

Abstract

Ligand-induced protein degradation has emerged as a compelling approach to promote the targeted elimination of proteins from cells by directing these proteins to the ubiquitin-proteasome machinery. So far, only a limited number of E3 ligases have been found to support ligand-induced protein degradation, reflecting a dearth of E3-binding compounds for proteolysis-targeting chimera (PROTAC) design. Here, we describe functional screening strategy performed with a focused library of candidate electrophilic PROTACs to discover bifunctional compounds that degrade proteins in human cells by covalently engaging E3 ligases. Mechanistic studies revealed that the electrophilic PROTACs act through modifying specific cysteines in DCAF11, a poorly characterized E3 ligase substrate adaptor. We further show that DCAF11-directed electrophilic PROTACs can degrade multiple endogenous proteins, including FBKP12 and the androgen receptor in human prostate cancer cells. Our findings designate DCAF11 as an E3 ligase capable of supporting ligand-induced protein degradation via electrophilic PROTACs.

Introduction

Small molecules are typically thought to produce pharmacological effects through directly impacting the function of proteins, for instance, by inhibiting the catalytic activity of an enzyme or stimulating the activity of a receptor. With increasing frequency, however, chemical probes and drugs are being discovered that act by promoting the degradation of proteins. Ligand-induced protein degradation often involves the formation of ternary complexes where small molecules serve as bridges that bring protein targets into close physical proximity of E3 ubiquitin ligases, which then ubiquitinate the protein targets leading to their proteolytic degradation by the proteasome[1–3]. Multiple categories of compounds have been found to act in this manner, including monofunctional degraders, or

*To whom correspondence should be addressed: zhangx@scripps.edu, cravatt@scripps.edu.

Supporting Information. Figures S1–12, Tables S1–S5, Materials and Methods, Synthetic Chemistry.

"molecular glues", and bifunctional degraders, or PROTACs (PROTeolysis TArgeting Chimeras)[4]. Ligand-induced protein degradation has advantages over more traditional small-molecule antagonism, in particular, for multi-domain proteins where antagonists may only block one of several functions (e.g., catalytic, but not scaffolding functions), while degraders instead promote the complete loss of the protein from the cell. Small-molecule degraders also have the potential to act catalytically in cells[5] and to confer functional outcomes to 'silent' ligand-binding sites[6]. The latter attribute holds potential for substantially increasing the druggability of the human proteome.

Key to the success of ligand-induced protein degradation is the identification of small molecules that bind to functional sites on E3 ligases[7]. So far, compounds capable of serving as mono- and/or bi-functional degraders have been discovered for only a limited number of E3 ligases, most prominently, cereblon (CRBN) and VHL[5, 8]. We and others have more recently identified a distinct category of electrophilic PROTACs that operate by covalently modifying E3 ligases, such as DCAF16, RNF4, and RNF114[9–11]. In the case of DCAF16, electrophilic PROTACs were found to promote ligand-induced protein degradation in a nuclear-restricted manner and at low stoichiometric engagement of the E3 ligase[11], reflecting the nuclear localization of DCAF16 and the covalent mechanism of electrophilic PROTACs, respectively.

DCAF16 was discovered to support ligand-induced protein degradation using PROTACs bearing a broadly reactive electrophilic fragment tested in HEK293T cells. Here, we hypothesized that, by testing an expanded library of bifunctional electrophilic compounds across a broader panel of human cancer cell lines, we may identify additional E3 ligases that support ligand-induced protein degradation. Our screen identified multiple electrophilic PROTACs that degraded the test protein FKBP12 in cancer cells, including a subset that were found by chemical proteomics to act through the substrate adaptor protein DCAF11. We demonstrate that electrophilic PROTACs acting through DCAF11 can also degrade the androgen receptor in 22Rv1 human prostate cancer cells. Finally, mechanistic studies indicate that electrophilic PROTACs engage specific cysteines in DCAF11, including a highly conserved residue C460, to promote ligand-induced protein degradation.

Results and Discussion

A cell-based screen to identify electrophilic PROTACs that degrade FKBP12.

We prepared a focused library of candidate electrophilic PROTACs bearing an SLF (Synthetic Ligand of FKBP) ligand for binding to the FKBP12 protein[12] coupled through a polyethylene glycol (PEG) linker to a structurally varied (mostly α-chloroacetamide (α-CA)) electrophilic group. To access structural diversity with facile chemistry, we leveraged the Ugi reaction[13] to produce ~20 SLF-α-CA bifunctional compounds. We used a variety of aldehydes and isocyanides as reaction partners in the Ugi reaction to yield a library that included aliphatic saturated hydrocarbons (e.g. 7-SLF, 16-SLF), saturated heterocycles (e.g. 11-SLF, 15-SLF), heteroaromatics (e.g. 8-SLF, 18-SLF, 20-SLF), electron poor aromatics (e.g. 10-SLF, 21-SLF) and electron rich aromatics (e.g. 17-SLF). This set of compounds, along with five previously reported compounds[11] (Figure S1), were screened in four human cancer cell lines from different tumors of origin (non-small cell lung cancer: H1975, H2122;

prostate cancer: 22Rv1; and pancreatic cancer: BxPC-3), an approach that we hoped would increase our probability of discovering active PROTACs by accessing diverse cellular proteomes. These cell lines were engineered to stably express cytosolic or nuclear localized FKBP12 fused to firefly luciferase (Luc-FKBP12, Figure 1A and Figure S2). Cells were exposed to compounds at 2 μM for 8 h and then evaluated for FKBP12 protein content by measuring firefly luciferase activity normalized to cell viability measurements (to account for potential cell toxicity effects of compounds; Table S1). Compounds that produced > 50% loss of cytosolic and/or nuclear FKBP12 were considered of potential interest. Lenalidomide-SLF (Len-SLF, Figure S1), a bifunctional compound that recruits CRBN for FKBP12 degradation[11], was used as a positive control and induced substantial loss of both cytosolic and nuclear FKBP12 in all four cell lines (Figure 1B). The candidate electrophilic PROTAC library exhibited diverse activity, including compounds that i) decreased both cytosolic and nuclear FBKP12 predominantly in a single cell line (e.g., 10-SLF, 17-SLF, 21-SLF), ii) decreased FKBP12 in multiple cell lines (e.g., 3-SLF), iii) decreased nuclear, but not cytosolic FKBP12 (including 22S, which was previously shown to degrade nuclear proteins in a DCAF16-dependent manner[11]); and iv) exhibited negligible effects on FKBP12 (e.g., 1-SLF, 6-SLF, 18-SLF) (Figure 1B).

Intrigued by the activity of the structurally related compounds 10-SLF and 21-SLF (Figure 1C and Figure S1), which caused the loss of Luc-FKBP12 in 22Rv1 cells, but not other tested cell lines (Figure 1B), we selected 21-SLF for further investigation. We first confirmed 21-SLF-induced loss of FKBP12 in 22Rv1 cells by Western blot analysis (Figure 1D), using the structurally related inactive compound 18-SLF as a control (Figure 1C, D). The reduction in FKBP12 caused by 21-SLF was blocked by co-treating with free SLF, as well as by the proteasome inhibitor MG132 or the neddylation inhibitor MLN4924 (Figure 2A), indicating the involvement of a Cullin-RING E3 ligase in the ligand-induced degradation mechanism[15]. Also supportive of this conclusion, 21-SLF induced the polyubiquitination of cytosolic and nuclear FKBP12 (Figure 2B). Degradation of FKBP12 was not observed with an analogue of 21-SLF where the electrophilic α-CA group was replaced with an unreactive propanamide (C-21-SLF, Figure S3), supporting that the mechanism of action of 21-SLF involves covalent modification of one or more proteins. We next pursued the identification of the E3 ligase that mediated 21-SLF-induced degradation of FBKP12.

21-SLF-induced degradation of FKBP12 is mediated by DCAF11.

We next employed a previously described proteomic approach[11] to identify proteins that co-immunoprecipitated with FLAG-tagged FKBP12 from 22Rv1 cells treated with 21-SLF (10 μM, 2 h). Among the proteins that were substantially enriched (> 4-fold) in immunoprecipitations of both cytosolic and nuclear FKBP12 from 21-SLF-treated versus DMSO-treated control cells were a single substrate receptor component of Cullin-RING E3 ligases – DCAF11 – and an additional Cullin-RING E3 component, DDB1 (Figure 3A and Table S2).

DCAF11 (or WDR23) has been implicated in the degradation of several proteins, including the transcription factor NRF2 (UniProt: Q16236)[16], the stem-loop binding protein SLBP

(UniProt: Q14493) and p21 (UniProt: P38936) during the cell cycle[17–18], and KAP1 (UniProt: Q13263) to regulate telomere length[19]. To our knowledge, small molecule ligands have not been described for DCAF11. To test whether DCAF11 was responsible for mediating 21-SLF-induced degradation of FKBP12, we used CRISPR/Cas9 methods to create DCAF11-knockout (KO) 22Rv1 cells (Figure S4A). These KO cells were generated as populations to minimize the potential for clonal effects on subsequent studies. Mass spectrometry (MS)-based proteomic experiments confirmed substantial loss of the targeted E3 ligase in the respective KO populations (> 70% loss of DCAF11 in DCAF11-KO cells) (Figure S4B, C and Table S3). 21-SLF caused the concentration-dependent (Figure 3B) and time-dependent (Figure S4D) degradation of both cytosolic and nuclear FKBP12 in DCAF11-WT, but not in DCAF11-KO 22Rv1 cells. Additionally, recombinant expression of HA-tagged DCAF11 restored 21-SLF-induced FKBP12 degradation in DCAF11-KO cells (Figure 3C). We furthermore found that HA-tagged DCAF11 co-immunoprecipitated with and mediated polyubiquitination of both cytosolic and nuclear FLAG-FKBP12 in the presence of 21-SLF and MG132 (Figure 3D), supporting the formation of a ternary complex involving 21-SLF, DCAF11, and FKBP12 in HEK293T cells. We finally analyzed 21-SLF-treated WT and DCAF11-KO 22Rv1 cells by MS-based proteomics, which confirmed selective degradation of endogenous FKBP12 in WT, but not DCAF11-KO cells (Figure 3E and Table S4). One additional protein, GSTO1 was decreased by 21-SLF in both WT and DCAF11-KO 22Rv1 cells (Figure 3D). GSTO1 harbors a highly reactive catalytic cysteine (Cys32)[20–21], which has been previously shown to be liganded by diverse α-CA compounds[20, 22]. We therefore speculate that 21-SLF may directly modify C32 in GSTO1, leading to destabilization of the protein.

KB02-SLF is a previous reported PROTAC that degrades FKBP12 in an DCAF16-dependent manner[11].

Having identified DCAF11 as an E3 ligase responsible for mediating the degradation of FKBP12 by 21-SLF, we wondered whether other screening hits from the electrophilic PROTAC library might also act through DCAF11. A representative subset of active and inactive compounds (Figure 1B) was evaluated for inducing FKBP12 degradation in DCAF11-WT and DCAF11-KO 22Rv1 cells. Interestingly, while several of the screening hits, including compounds with structural similarity to 21-SLF (e.g., 10-SLF), also degraded FKBP12 in a DCAF11-dependent manner, one candidate electrophilic PROTAC 3-SLF maintained activity in DCAF11-KO cells, pointing to a different mechanism of action (Figure 3F).

DCAF11 cysteines involved in 21-SLF-induced degradation of FKBP12.

The α-CA electrophile found in 21-SLF mainly reacts with cysteine among the proteinaceous amino acids[23]. We initially searched our internal and published chemical proteomic datasets of α-CA-sensitive cysteines[20–21, 24], in the hopes of identifying candidate cysteines in DCAF11 that might be liganded by this electrophilic group. However, the coverage of DCAF11 cysteines in these datasets was limited and did not reveal obvious sites of α-CA-sensitivity. We therefore pursued an alternative approach of expressing WT and individual C-to-A mutants of DCAF11 alongside Luc-FKBP12 in HEK293T cells and

monitoring 21-SLF-induced loss of FKBP12. We first confirmed that both cytosolic and nuclear Luc-FKBP12 were degraded by 21-SLF in a concentration-dependent and MLN4924-sensitive manner in WT-DCAF11-expressing HEK293T cells, but not in HEK293T cells expressing only Luc-FKBP12 (Figure 4A, B). The expression of C-to-A mutants of DCAF11 in HEK293T cells (Figure S5) revealed that none of the individual cysteine mutations completely abolished FKBP12 degradation by 21-SLF; however, the C460A-DCAF11 mutant showed a partial impairment in FKBP12 degradation (Figure 4C). We next combined the C460A mutation with other C-to-A mutations to create double mutant DCAF11 variants, but none of these double mutants showed further impairment in 21-SLF-induced degradation of FKBP12 (Figure 4C and Figure S5).

Our mutational analysis suggested that 21-SLF may promote FKBP12 through engaging multiple cysteines. Although the three-dimensional structure of DCAF11 has not yet been determined, a structure is available for the U5 subunit of human spliceosome (SNRNP40, pdb: 3JCR, Figure 4D), which shares a similar WDR domain to DCAF11. Sequence alignment between DCAF11 and U5–40K identified three cysteines in DCAF11 (C443, C460, and C485) that may be in close spatial proximity within the WDR domain (Figure 4D and Figure S6). Mutation of all three cysteines to alanine (C443A/C460A/C485A triple mutant; or DCAF11-3CA) completely blocked 21-SLF-induced degradation of FKBP12 (Figure 4E). We confirmed that DCAF11-WT and the DCAF11-3CA triple mutant bound to similar extents to DDB1 in cells (Figure S7), suggesting that the triple mutant protein retains a native conformation capable of engaging in Cullin-RING E3 complexes. We then used recombinant His-tagged FKBP12 protein and an anti-His antibody to visualize SLF-modified proteins in a far-western blot assay. This experiment demonstrated that FKBP12 bound to DCAF11-WT, but not the DCAF11-3CA triple mutant in 21-SLF treated cells (Figure S8), supporting that DCAF11 is covalently modified by 21-SLF on one or more of the three cysteines in DCAF11 (C443, C460, and C485). Interestingly, the C443A/C485A double mutant showed equivalent degradation activity to DCAF11-WT (Figure 4E). We interpret these data to indicate that C460 of DCAF11 is sufficient to mediate the full degradation activity of 21-SLF, but, in the absence of this cysteine, C443 and C485 can serve as additional engagement sites that support 21-SLF-induced protein degradation.

We next performed chemical proteomic experiments using an iodoacetamide-desthiobiotin (IA-DTB) probe to map cysteines that were substantially engaged by 21-SLF (10 μM, 2 h) in HA-DCAF11-transfected HEK293T cells. The results revealed that 21-SLF only engaged DCAF11_C460 to a limited extent (Table S5), which is consistent with a model where the compound supports targeted protein degradation at low fractional occupancy of DCAF11[11]. The chemical proteomic experiments also provided insights into the broader reactivity of 21-SLF, showing that, across > 12,000 quantified cysteines, the compound only substantially engaged (>50%) a handful of cysteines – GSTO1_C32, PTGES2_C110, VSNL1_C187, MGST3_C62, HMOX2_C265 and HMOX2_C282 (Figure S9 and Table S5). Considering that 21-SLF promoted reductions in GSTO1 protein content by a DCAF11-independent mechanism in cells (Figure 3E), these data suggest that direct engagement of C32 by electrophilic compounds may destabilize GSTO1.

DCAF11-dependent degradation of the androgen receptor.

We finally investigated whether electrophilic PROTACs acting through DCAF11 could degrade an additional endogenous protein beyond FKBP12. The 22Rv1 cells in which DCAF11-dependent ligand-induced degradation activity was discovered express the androgen receptor (AR), which is an oncogenic transcription factor important for prostate cancer growth and a target of interest in several previous PROTAC studies[25–27]. We synthesized a candidate electrophilic PROTAC 21-ARL bearing the α-CA group found in 21-SLF coupled through a PEG linker to a previously defined AR ligand[26–27] (Figure 5A). 21-ARL treatment for 8 h caused the concentration-dependent degradation of AR in WT cells, but not DCAF11-KO 22Rv1 cells (Figure 5B). At 10 μM, 21-ARL led to 90% loss of AR (Figure 5B). 22Rv1 cells also express a splice variant of AR, AR-V7, that lacks the ligand-binding domain[28–29], and the abundance of this variant was not affected by 21-ARL treatment (Figure 5B and Figure S10), consistent with its lack of response to other AR-directed PROTACs[30–31].

These data indicate that electrophilic PROTACs engaging DCAF11 can promote the degradation of multiple endogenous proteins (FKBP12, AR) in human cells.

Conclusion

As interest in ligand-induced protein degradation has intensified, so has the pursuit of E3 ligases that can be targeted by small molecules to mediate this event-driven pharmacology[7, 32]. Examples of E3 ligases that have recently been shown to support ligand-induced protein degradation include DCAF16, RNF4, RNF114 and KEAP1[9–11, 33]. Here, we used a cell-based screening approach combined with chemical proteomics to identify DCAF11 as an E3 ligase that mediates ligand-induced protein degradation when engaged by electrophilic PROTACs. While we discovered DCAF11 using electrophilic PROTACs that showed activity in 22Rv1 cells, but not other tested cell lines, we are unsure of the mechanistic basis for this cell type-restricted profile. DCAF11 itself appears to be expressed in all of the tested cell lines, albeit at higher abundance in 22Rv1 cells[34] (Figure S11), which could point to a threshold quantity of the E3 ligase required to observe protein degradation effects. Potentially consistent with this hypothesis, recombinant expression of DCAF11 conferred strong ligand-induced protein degradation activity to HEK293T cells (Figure 4A, B). We observed higher hit rate in 22Rv1 cells compared to other cells. Besides the possibility that DCAF11 is expressed at higher abundance in 22Rv1 cells, which might contribute to the higher hit rate, 22Rv1 cells may also have a higher overall capacity to support ligand-induced protein degradation due to higher cell permeability or lower cellular glutathione (GSH) concentration/reactivity, which are hypotheses we hope to explore in the future..

Mechanistic studies suggest that multiple cysteines in DCAF11, possibly colocalized on the same surface of the protein, can mediate protein degradation by electrophilic PROTACs. The apparent sufficiency of C460, however, suggests future efforts could focus on creating more potent and selective covalent ligands for this cysteine in DCAF11. We also note that C460, unlike C443 and C485, is highly conserved across DCAF11 orthologues from other species, including mammals, flies, worms, and fish (Figure S8). We therefore wonder if C460 might

be a site for endogenous electrophile action to shape the substrate scope of DCAF11-mediated protein degradation in response to, for instance, oxidative stress in cells.

In our previous studies of DCAF16, we found that only a minor fraction (10–40%) of the protein needed to be engaged by electrophilic PROTACs to produce robust targeted protein degradation outcomes[11]. Technically speaking, our stoichiometry estimates for DCAF16 engagement by electrophilic PROTACs could be conveniently measured by shifts in the migration of this protein by SDS-PAGE. DCAF11, being a much larger protein than DCAF16 (62 vs 24 kDa), did not show a clear gel-shift following electrophilic PROTAC treatment. And, we also found that C460, as well as C443 and C485, of endogenous DCAF11 have been rarely quantified in past chemical proteomic experiments of cysteine reactivity. Here, we did observe that 21-SLF only showed modest (~10%) engagement of DCFA11_C460 at pharmacologically relevant concentrations (10 μM) in cells recombinantly expressing DCAF11 (Table S5), although whether this low stoichiometry reflects the degree of engagement of endogenous DCAF11 by 21-SLF remains unknown. Going forward, the stoichiometry of DCAF11 cysteine engagement by electrophilic PROTACs may be measurable using targeted proteomic methods, which should have enhanced sensitivity[35]. Understanding DCAF11 cysteine engagement would help to clarify whether electrophilic PROTACs can act through this protein with minimal perturbations to its endogenous functions, as might be possible at sub-stoichiometric interactions. We did observe two previously described endogenous substrates of DCAF11 in our proteomic experiments – SLBP and KAP1 – and neither were altered in abundance in 21-SLF-treated cells (Table S3).

Projecting forward, we are generally interested in the potential of the screening approach described herein to discover additional E3 ligases that can be targeted by electrophilic PROTACs. We note that other tested compounds showed cell type-related degradation profiles that differed from 21-SLF (e.g., 3-SLF; Figure 1B) and retained activity in DCAF11-KO cells (Figure 3F). Understanding the E3 ligase interactions for such compounds is an important future objective. We also only screened a modest number of candidate electrophilic PROTACs and increasing the content and structural diversity of this compound library may facilitate discovery of additional E3 ligases amenable to electrophilic PROTAC action. We should, however, qualify that further optimization of the potency and selectivity of electrophilic PROTACs acting through DCAF11 is needed to furnish more advanced chemical probes. In this regard, the electrophilic component of the PROTACs possesses a chiral center, and since these compounds were tested herein as epimeric mixtures, it will be important in future studies to determine if they show stereoselective degradation activity. Also, while α-CAs can serve as valuable initial tool compounds for probing the functions of proteins in cells, the identification of more tempered electrophiles (e.g., acrylamides, butynamides) capable of targeting DCAF11 would enable investigation of the broader potential for this E3 ligase to contribute to the field of ligand-induced protein degradation. It is nonetheless encouraging that first-generation electrophilic PROTACs acting through DCAF11 were capable of promoting the degradation of multiple endogenous proteins, including AR, an important prostate cancer drug target. Our findings, combined with other recent studies[9–11, 33], underscore the value of incorporating covalent chemistry into PROTAC design to expand the scope of E3 ligases that mediate ligand-induced protein degradation.

Supplementary Material

Refer to Web version on PubMed Central for supplementary material.

Acknowledgements

We thank Yongfeng Tao for helpful discussions. This work was supported by the National Institutes of Health CA231991 (B.F.C.) and CA212467 (V.M.C.). X.Z. was supported by the National Cancer Institute of the National Institutes of Health under Award Number K99CA248715 and the Damon-Runyon Cancer Research Foundation (DRG-2341-18).

References

1. Bondeson DP; Crews CM, Targeted Protein Degradation by Small Molecules. Annu Rev Pharmacol Toxicol 2017, 57, 107–123. [PubMed: 27732798]
2. Schapira M; Calabrese MF; Bullock AN; Crews CM, Targeted protein degradation: expanding the toolbox. Nat Rev Drug Discov 2019, 18 (12), 949–963. [PubMed: 31666732]
3. Kostic M; Jones LH, Critical Assessment of Targeted Protein Degradation as a Research Tool and Pharmacological Modality. Trends Pharmacol Sci 2020, 41 (5), 305–317. [PubMed: 32222318]
4. Chamberlain PP; Hamann LG, Development of targeted protein degradation therapeutics. Nat Chem Biol 2019, 15 (10), 937–944. [PubMed: 31527835]
5. Bondeson DP; Mares A; Smith IE; Ko E; Campos S; Miah AH; Mulholland KE; Routly N; Buckley DL; Gustafson JL; Zinn N; Grandi P; Shimamura S; Bergamini G; Faelth-Savitski M; Bantscheff M; Cox C; Gordon DA; Willard RR; Flanagan JJ; Casillas LN; Votta BJ; den Besten W; Famm K; Kruidenier L; Carter PS; Harling JD; Churcher I; Crews CM, Catalytic in vivo protein knockdown by small-molecule PROTACs. Nat Chem Biol 2015, 11 (8), 611–7. [PubMed: 26075522]
6. Raina K; Crews CM, Targeted protein knockdown using small molecule degraders. Curr Opin Chem Biol 2017, 39, 46–53. [PubMed: 28605671]
7. Ishida T; Ciulli A, E3 Ligase Ligands for PROTACs: How They Were Found and How to Discover New Ones. SLAS Discov 2020, 2472555220965528.
8. Winter GE; Buckley DL; Paulk J; Roberts JM; Souza A; Dhe-Paganon S; Bradner JE, DRUG DEVELOPMENT. Phthalimide conjugation as a strategy for in vivo target protein degradation. Science 2015, 348 (6241), 1376–81. [PubMed: 25999370]
9. Ward CC; Kleinman JI; Brittain SM; Lee PS; Chung CYS; Kim K; Petri Y; Thomas JR; Tallarico JA; McKenna JM; Schirle M; Nomura DK, Covalent Ligand Screening Uncovers a RNF4 E3 Ligase Recruiter for Targeted Protein Degradation Applications. ACS Chem Biol 2019, 14 (11), 2430–2440. [PubMed: 31059647]
10. Spradlin JN; Hu X; Ward CC; Brittain SM; Jones MD; Ou L; To M; Proudfoot A; Ornelas E; Woldegiorgis M; Olzmann JA; Bussiere DE; Thomas JR; Tallarico JA; McKenna JM; Schirle M; Maimone TJ; Nomura DK, Harnessing the anti-cancer natural product nimbolide for targeted protein degradation. Nat Chem Biol 2019, 15 (7), 747–755. [PubMed: 31209351]
11. Zhang X; Crowley VM; Wucherpfennig TG; Dix MM; Cravatt BF, Electrophilic PROTACs that degrade nuclear proteins by engaging DCAF16. Nat Chem Biol 2019, 15 (7), 737–746. [PubMed: 31209349]
12. Amara JF; Clackson T; Rivera VM; Guo T; Keenan T; Natesan S; Pollock R; Yang W; Courage NL; Holt DA; Gilman M, A versatile synthetic dimerizer for the regulation of protein-protein interactions. Proc Natl Acad Sci U S A 1997, 94 (20), 10618–23. [PubMed: 9380684]
13. Tempest PA, Recent advances in heterocycle generation using the efficient Ugi multiple-component condensation reaction. Curr Opin Drug Discov Devel 2005, 8 (6), 776–88.
14. Welsch ME; Snyder SA; Stockwell BR, Privileged scaffolds for library design and drug discovery. Curr Opin Chem Biol 2010, 14 (3), 347–61. [PubMed: 20303320]
15. Soucy TA; Smith PG; Milhollen MA; Berger AJ; Gavin JM; Adhikari S; Brownell JE; Burke KE; Cardin DP; Critchley S; Cullis CA; Doucette A; Garnsey JJ; Gaulin JL; Gershman RE; Lublinsky AR; McDonald A; Mizutani H; Narayanan U; Olhava EJ; Peluso S; Rezaei M; Sintchak MD;

Talreja T; Thomas MP; Traore T; Vyskocil S; Weatherhead GS; Yu J; Zhang J; Dick LR; Claiborne CF; Rolfe M; Bolen JB; Langston SP, An inhibitor of NEDD8-activating enzyme as a new approach to treat cancer. Nature 2009, 458 (7239), 732–6. [PubMed: 19360080]

16. Lo JY; Spatola BN; Curran SP, WDR23 regulates NRF2 independently of KEAP1. PLoS Genet 2017, 13 (4), e1006762. [PubMed: 28453520]
17. Chen Z; Wang K; Hou C; Jiang K; Chen B; Chen J; Lao L; Qian L; Zhong G; Liu Z; Zhang C; Shen H, CRL4B(DCAF11) E3 ligase targets p21 for degradation to control cell cycle progression in human osteosarcoma cells. Sci Rep 2017, 7 (1), 1175. [PubMed: 28446751]
18. Djakbarova U; Marzluff WF; Koseoglu MM, DDB1 and CUL4 associated factor 11 (DCAF11) mediates degradation of Stem-loop binding protein at the end of S phase. Cell Cycle 2016, 15 (15), 1986–96. [PubMed: 27254819]
19. Le R; Huang Y; Zhang Y; Wang H; Lin J; Dong Y; Li Z; Guo M; Kou X; Zhao Y; Chen M; Zhu Q; Zhao A; Yin J; Sun J; Su Z; Shi K; Gao Y; Chen J; Liu W; Kang L; Wang Y; Li C; Liu X; Gao R; Wang H; Ju Z; Gao S, Dcaf11 activates Zscan4-mediated alternative telomere lengthening in early embryos and embryonic stem cells. Cell Stem Cell 2020.
20. Backus KM; Correia BE; Lum KM; Forli S; Horning BD; Gonzalez-Paez GE; Chatterjee S; Lanning BR; Teijaro JR; Olson AJ; Wolan DW; Cravatt BF, Proteome-wide covalent ligand discovery in native biological systems. Nature 2016, 534 (7608), 570–4. [PubMed: 27309814]
21. Bar-Peled L; Kemper EK; Suciu RM; Vinogradova EV; Backus KM; Horning BD; Paul TA; Ichu TA; Svensson RU; Olucha J; Chang MW; Kok BP; Zhu Z; Ihle NT; Dix MM; Jiang P; Hayward MM; Saez E; Shaw RJ; Cravatt BF, Chemical Proteomics Identifies Druggable Vulnerabilities in a Genetically Defined Cancer. Cell 2017, 171 (3), 696–709 e23. [PubMed: 28965760]
22. Kambe T; Correia BE; Niphakis MJ; Cravatt BF, Mapping the protein interaction landscape for fully functionalized small-molecule probes in human cells. J Am Chem Soc 2014, 136 (30), 10777–82. [PubMed: 25045785]
23. Weerapana E; Simon GM; Cravatt BF, Disparate proteome reactivity profiles of carbon electrophiles. Nat Chem Biol 2008, 4 (7), 405–7. [PubMed: 18488014]
24. Vinogradova EV; Zhang X; Remillard D; Lazar DC; Suciu RM; Wang Y; Bianco G; Yamashita Y; Crowley VM; Schafroth MA; Yokoyama M; Konrad DB; Lum KM; Simon GM; Kemper EK; Lazear MR; Yin S; Blewett MM; Dix MM; Nguyen N; Shokhirev MN; Chin EN; Lairson LL; Melillo B; Schreiber SL; Forli S; Teijaro JR; Cravatt BF, An Activity-Guided Map of Electrophile-Cysteine Interactions in Primary Human T Cells. Cell 2020, 182 (4), 1009–1026 e29. [PubMed: 32730809]
25. Schneekloth AR; Pucheault M; Tae HS; Crews CM, Targeted intracellular protein degradation induced by a small molecule: En route to chemical proteomics. Bioorg Med Chem Lett 2008, 18 (22), 5904–8. [PubMed: 18752944]
26. Han X; Zhao L; Xiang W; Qin C; Miao B; Xu T; Wang M; Yang CY; Chinnaswamy K; Stuckey J; Wang S, Discovery of Highly Potent and Efficient PROTAC Degraders of Androgen Receptor (AR) by Employing Weak Binding Affinity VHL E3 Ligase Ligands. J Med Chem 2019, 62 (24), 11218–11231. [PubMed: 31804827]
27. Han X; Wang C; Qin C; Xiang W; Fernandez-Salas E; Yang CY; Wang M; Zhao L; Xu T; Chinnaswamy K; Delproposto J; Stuckey J; Wang S, Discovery of ARD-69 as a Highly Potent Proteolysis Targeting Chimera (PROTAC) Degrader of Androgen Receptor (AR) for the Treatment of Prostate Cancer. J Med Chem 2019, 62 (2), 941–964. [PubMed: 30629437]
28. Hu R; Dunn TA; Wei S; Isharwal S; Veltri RW; Humphreys E; Han M; Partin AW; Vessella RL; Isaacs WB; Bova GS; Luo J, Ligand-independent androgen receptor variants derived from splicing of cryptic exons signify hormone-refractory prostate cancer. Cancer Res 2009, 69 (1), 16–22. [PubMed: 19117982]
29. Sharp A; Coleman I; Yuan W; Sprenger C; Dolling D; Rodrigues DN; Russo JW; Figueiredo I; Bertan C; Seed G; Riisnaes R; Uo T; Neeb A; Welti J; Morrissey C; Carreira S; Luo J; Nelson PS; Balk SP; True LD; de Bono JS; Plymate SR, Androgen receptor splice variant-7 expression emerges with castration resistance in prostate cancer. J Clin Invest 2019, 129 (1), 192–208. [PubMed: 30334814]
30. Salami J; Alabi S; Willard RR; Vitale NJ; Wang J; Dong H; Jin M; McDonnell DP; Crew AP; Neklesa TK; Crews CM, Androgen receptor degradation by the proteolysis-targeting chimera

ARCC-4 outperforms enzalutamide in cellular models of prostate cancer drug resistance. Commun Biol 2018, 1, 100. [PubMed: 30271980]

31. Raina K; Lu J; Qian Y; Altieri M; Gordon D; Rossi AM; Wang J; Chen X; Dong H; Siu K; Winkler JD; Crew AP; Crews CM; Coleman KG, PROTAC-induced BET protein degradation as a therapy for castration-resistant prostate cancer. Proc Natl Acad Sci U S A 2016, 113 (26), 7124–9. [PubMed: 27274052]
32. Lai AC; Crews CM, Induced protein degradation: an emerging drug discovery paradigm. Nat Rev Drug Discov 2017, 16 (2), 101–114. [PubMed: 27885283]
33. Tong B; Luo M; Xie Y; Spradlin JN; Tallarico JA; McKenna JM; Schirle M; Maimone TJ; Nomura DK, Bardoxolone conjugation enables targeted protein degradation of BRD4. Sci Rep 2020, 10 (1), 15543. [PubMed: 32968148]
34. Nusinow DP; Szpyt J; Ghandi M; Rose CM; McDonald ER 3rd; Kalocsay M; Jane-Valbuena J; Gelfand E; Schweppe DK; Jedrychowski M; Golji J; Porter DA; Rejtar T; Wang YK; Kryukov GV; Stegmeier F; Erickson BK; Garraway LA; Sellers WR; Gygi SP, Quantitative Proteomics of the Cancer Cell Line Encyclopedia. Cell 2020, 180 (2), 387–402 e16. [PubMed: 31978347]
35. Ebhardt HA; Root A; Sander C; Aebersold R, Applications of targeted proteomics in systems biology and translational medicine. Proteomics 2015, 15 (18), 3193–208. [PubMed: 26097198]

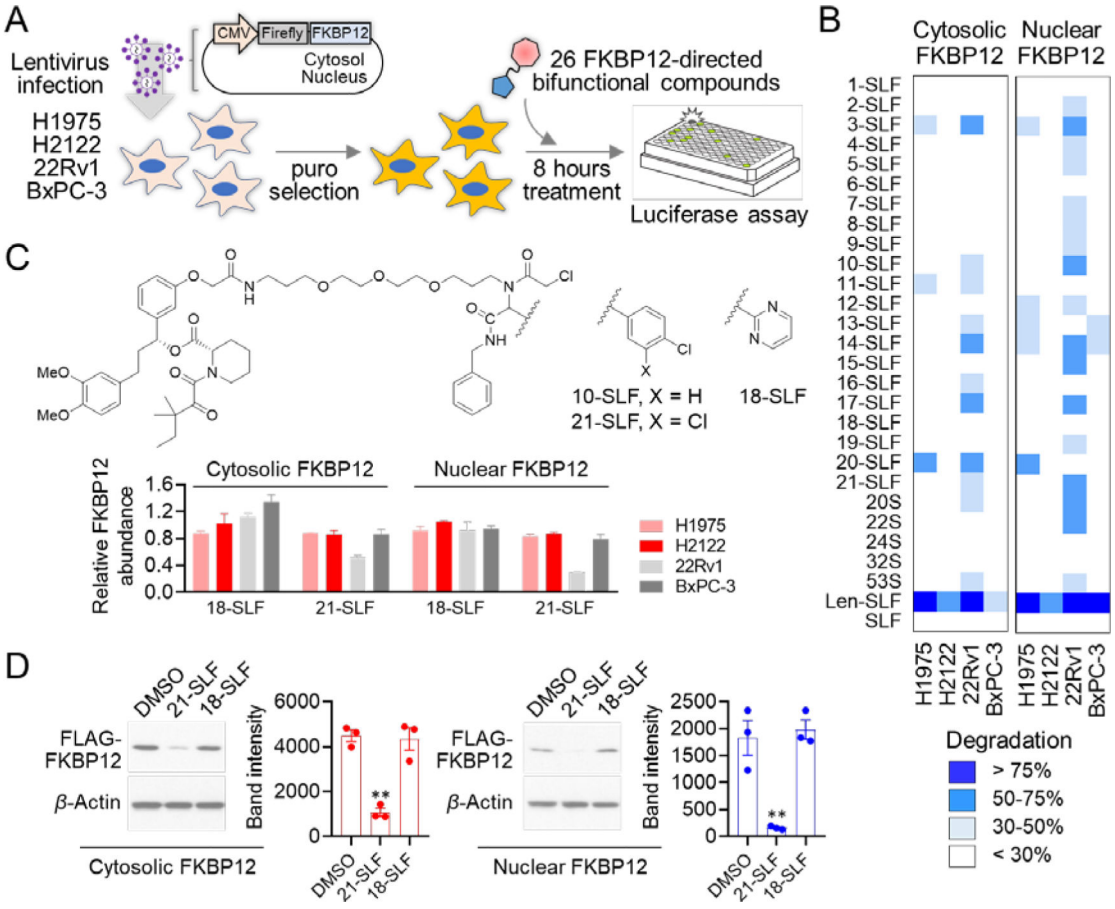

Figure 1. A cell-based screen to identify electrophilic PROTACs that degrade FKBP12.

A. Schematic depicting the strategy of screening candidate electrophilic PROTACs targeting the FKBP12 protein (either cytosol- or nuclear-localized) fused to a luciferase reporter (Luc-FKBP12). Cells were exposed to compounds at 2 μM for 8 h. Luciferase activity was normalized to cell viability measured by parallel CellTiter-Glo assays (Table S1). **B**. Heatmap showing the relative abundance of Luc-FKBP12 in cells treated with candidate electrophilic PROTACs compared to DMSO control. Data represent mean values (n = 2 biologically independent experiments). **C**. Structures of representative active (10-SLF, 21-SLF) and inactive (18-SLF) compounds from the screen. Bar graph (bottom) represents the screening data in **B** for 18-SLF and 21-SLF. Data are mean ± SD (n = 2). **D**. Confirmation of the activity of 21-SLF (2 μM, 8 h) by Western blotting of 22Rv1 cells stably expressing cytosolic or nuclear FLAG-tagged FKBP12. The result is representative of three biologically independent experiments. Bar graph (right) represents quantification of the FLAG-FKBP12 protein content. Data are mean values ± SEM (n = 3). Statistical significance was calculated with unpaired two-tailed Student's t-tests comparing 21-SLF-treated to DMSO or 18-SLF-treated cells. $^{**}P < 0.01$.

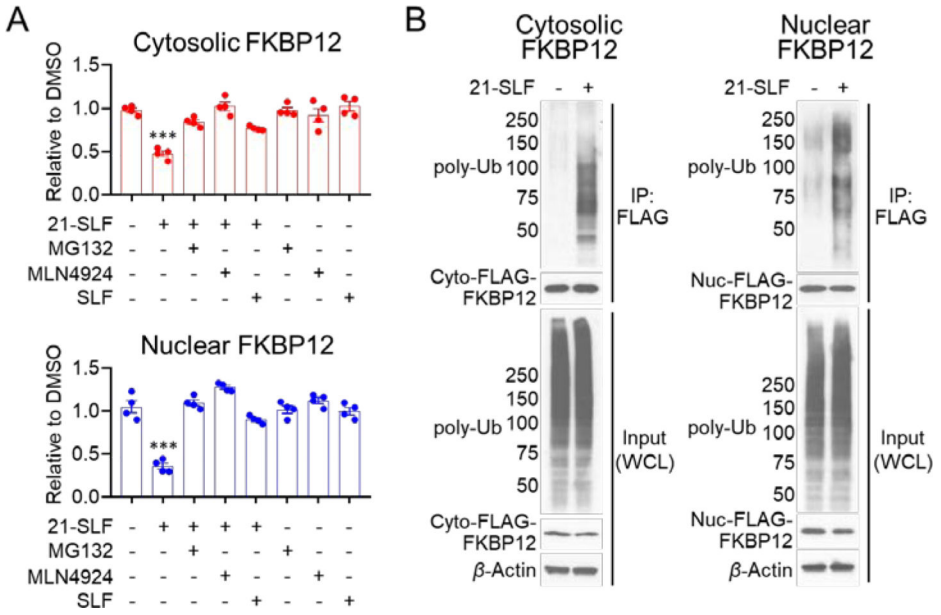

Figure 2. 21-SLF promotes proteasomal degradation of cytosolic and nuclear FKBP12 via the action of Cullin-RING ubiquitin ligase(s).

A. 21-SLF-mediated Luc-FKBP12 degradation is blocked by the proteasome inhibitor MG132 and the neddylation inhibitor MLN4924. 22Rv1 cells stably expressing cytosolic or nuclear Luc-FKBP12 were co-treated with 21-SLF (2 μM) and MG132 (10 μM) or MLN4924 (1 μM) for 8 h. Relative Luc-FKBP12 abundance was measured by luciferase signals in comparison to DMSO-treated control cells and normalized to cell viability. Data are mean values ± SEM (n = 4 biologically independent experiments). Statistical significance was calculated with unpaired two-tailed Student's t-tests comparing 21-SLF-treated to DMSO-treated cells. ***$P < 0.001$. **B**. 21-SLF induces polyubiquitination of cytosolic and nuclear FLAG-FKBP12 in 22Rv1 cells. 22Rv1 cells stably expressing cytosolic or nuclear FLAG-FKBP12 were treated with DMSO or 21-SLF (10 μM) in the presence of the proteasome inhibitor MG132 (10 μM) for 2 h. The result is representative of two biologically independent experiments.

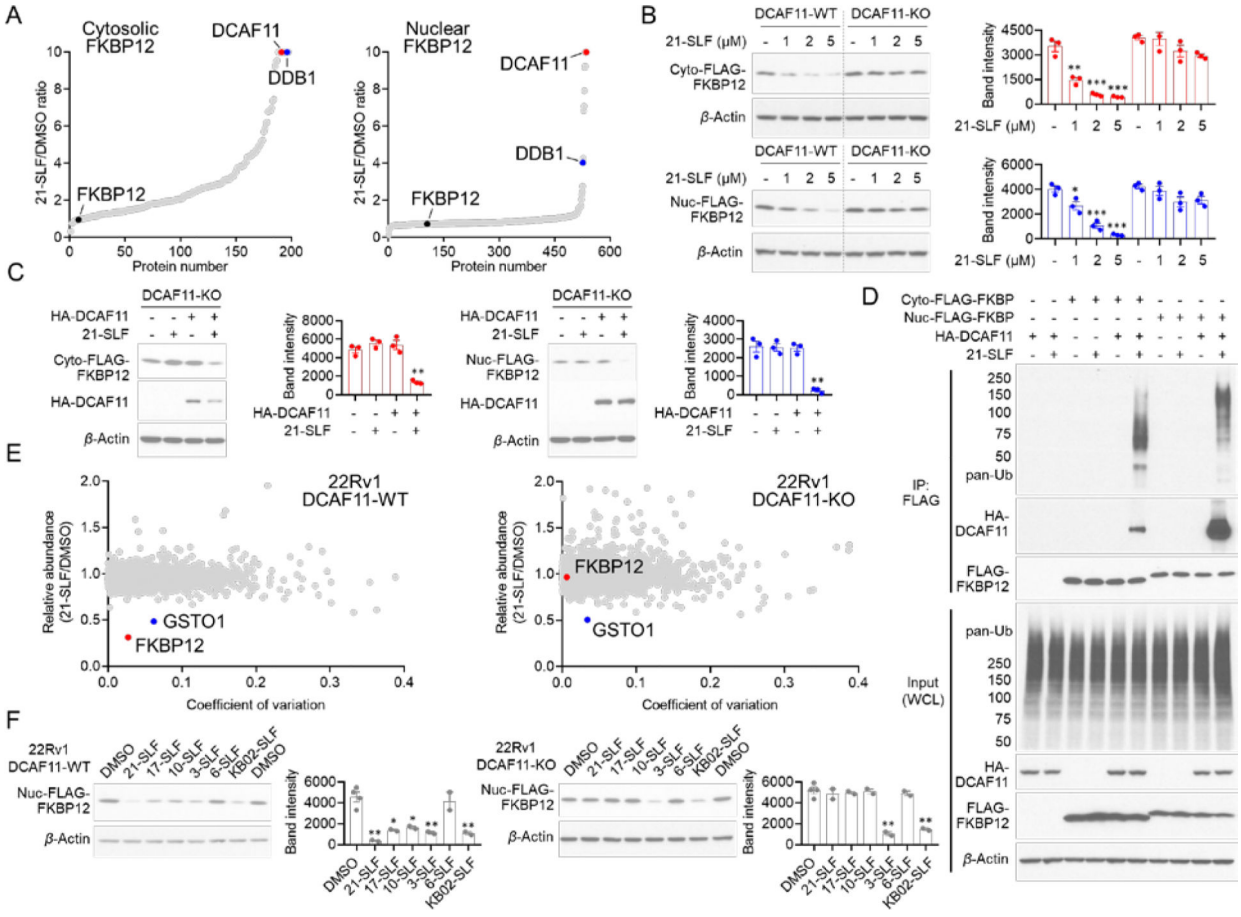

Figure 3. DCAF11 mediates 21-SLF-induced degradation of FKBP12.

A. Quantitative MS-based proteomics showing 21-SLF/DMSO ratio values of proteins identified in anti-FLAG affinity enrichment experiments, where a high ratio indicates proteins preferentially enriched from cells treated with 21-SLF (10 μM). The maximum 21-SLF/DMSO value was set as 10. 22Rv1 cells stably expressing cytosolic or nuclear FLAG-FKBP12 were treated with DMSO or 21-SLF (10 μM) in the presence of the proteasome inhibitor MG132 (10 μM) for 2 h. The y-axis and x-axis correspond to the average 21-SLF/DMSO ratio and protein number, respectively, from four biologically independent experiments. **B**. Concentration-dependent degradation of stably expressed cytosolic or nuclear FLAG-FKBP12 in DCAF11-WT and DCAF11-KO 22Rv1 cells following treatment with 21-SLF (1, 2, and 5 μM) for 8 h. The result is representative of three biologically independent experiments. Bar graph (right) represents quantification of the FLAG-FKBP12 protein content. Data are mean ± SEM (n = 3). Statistical significance was calculated with unpaired two-tailed Student's t-tests comparing 21-SLF-treated to DMSO-treated cells. $*P < 0.05$, $**P < 0.01$, $***P < 0.001$. **C**. Expression of HA-DCAF11 in DCAF11-KO 22Rv1 cells restored 21-SLF-mediated degradation of cytosolic and nuclear FLAG-FKBP12. 22Rv1 DCAF11-KO cells were transiently transfected with HA-DCAF11 or empty pRK5 vector and cytosolic or nuclear FLAG-FKBP12 for 24 h and then treated with 21-SLF (2 μM, 8 h). The result is a representative of three biologically independent experiments. Bar graph (right) represents quantification of the FLAG-FKBP12 protein content. Data are mean ±

SEM (n = 3). Statistical significance was calculated with unpaired two-tailed Student's t-tests comparing 21-SLF-treated HA-DCAF11-expressing cells to 21-SLF-treated DCAF11-KO cells. $^{**}P < 0.01$. **D**. DCAF11 interacted with and mediated polyubiquitination of cytosolic and nuclear FKBP12 in the presence of 21-SLF. HEK293T cells were transiently transfected with HA-DCAF11 and cytosolic or nuclear FLAG-FKBP12 for 24 h and then treated with DMSO or 21-SLF (10 μM, 2 h) in the presence of MG132 (10 μM). The result is representative of two experiments (n = 2 biologically independent experiments). **E**. Quantitative MS-based proteomics comparing protein abundance profiles of DCAF11-WT and DCAF11-KO 22Rv1 cells treated with DMSO or 21-SLF (10 μM) for 8 h. The y-axis and x-axis correspond to the average relative abundance (21-SLF/DMSO) and coefficient of variation, respectively, from two biologically independent experiments. **F**. Degradation of stably expressed nuclear FLAG-FKBP12 in DCAF11-WT and DCAF11-KO 22Rv1 cells following treatment with the indicated compounds (2 μM for KB02-SLF and 10 μM for the others, 8 h). The result is a representative of two biologically independent experiments. Bar graph (right) represents quantification of the FLAG-FKBP12 protein content. Data are mean ± SD (n = 4 for DMSO treatment, n = 2 for others). Statistical significance was calculated with unpaired two-tailed Student's t-tests comparing DMSO-treated to compound-treated cells. $^{*}P < 0.05$, $^{**}P < 0.01$.

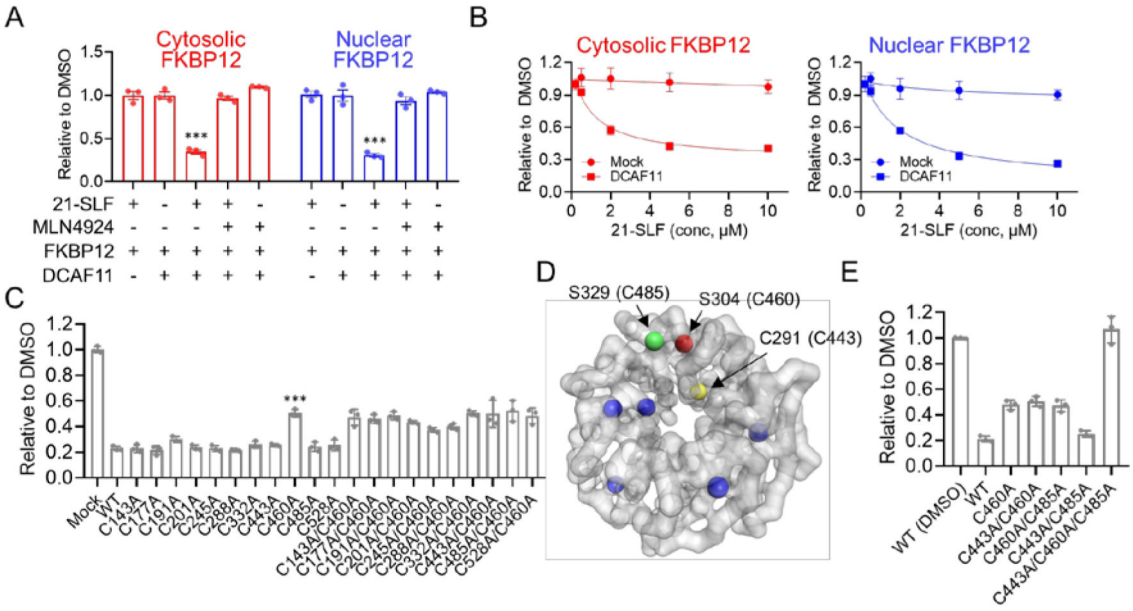

Figure 4. Evaluation of DCAF11 cysteines involved in 21-SLF-induced degradation of FKBP12.

A. 21-SLF-mediated degradation of cytosolic and nuclear Luc-FKBP12 in HEK293T cells co-expressing HA-DCAF11. HEK293T cells were transfected with HA-DCAF11 and cytosolic or nuclear Luc-FKBP12 for 24 h and then co-treated with 21-SLF (10 μM) and DMSO or MLN4924 1 μM) for 8 h. Luc-FKBP12 abundance was measured by luciferase signals in comparison to DMSO-treated control cells and normalized to cell viability. Data are mean ± SEM (n = 3 biologically independent experiments). Statistical significance was calculated with unpaired two-tailed Student's t-tests comparing 21-SLF-treated and DMSO-treated HA-DCAF11/Luc-FKBP12-co-expressing cells. ***$P < 0.001$. **B**. Concentration-dependent degradation of cytosolic or nuclear Luc-FKBP12 in HEK293T cells co-expressing Luc-FKBP12 and HA-DCAF11. HEK293T cells were transfected with HA-DCAF11 or pRK5 empty vector and cytosolic or nuclear Luc-FKBP12 for 24 h and then treated with 21-SLF (0.2, 0.5, 2, 5 and 10 μM) for 8 h. Luc-FKBP12 abundance was measured as in panel **A**. Data are mean ± SEM (n = 3 biologically independent experiments). **C**. Evaluation of DCAF11 cysteines that support 21-SLF-mediated Luc-FKBP12 degradation. HEK293T cells were transfected with the indicated C-to-A mutants of HA-DCAF11 and nuclear Luc-FKBP12 for 24 h and then treated with 21-SLF (10 μM, 8 h). Luc-FKBP12 abundance was measured as in panel **A**. Data are mean ± SEM (n = 3 biologically independent experiments). Statistical significance was calculated with unpaired two-tailed Student's t-tests comparing DCAF11-WT and DCAF11-C460A. ***$P < 0.001$. **D**. Cryo-electron microscopy structure of SNRNP40, the U5 subunit of human spliceosome (pdb: 3JCR). C291, S304 and S329 in SNRNP40 correspond to C443, C460 and C485 in DCAF11 based on sequence alignment (Figure S5). Blue highlighted amino acids correspond to the predicted locations of other cysteines in DCAF11. **E**. Evaluation of DCAF11 cysteines that support 21-SLF-mediated Luc-FKBP12 degradation. HEK293T cells were transfected with the indicated C-to-A mutants of HA-DCAF11 and nuclear Luc-FKBP12 for 24 h and then treated with 21-SLF (10 μM, 8 h). Luc-FKBP12 abundance was

measured as in panel **A**. Data are mean ± SEM (n = 3 biologically independent experiments).

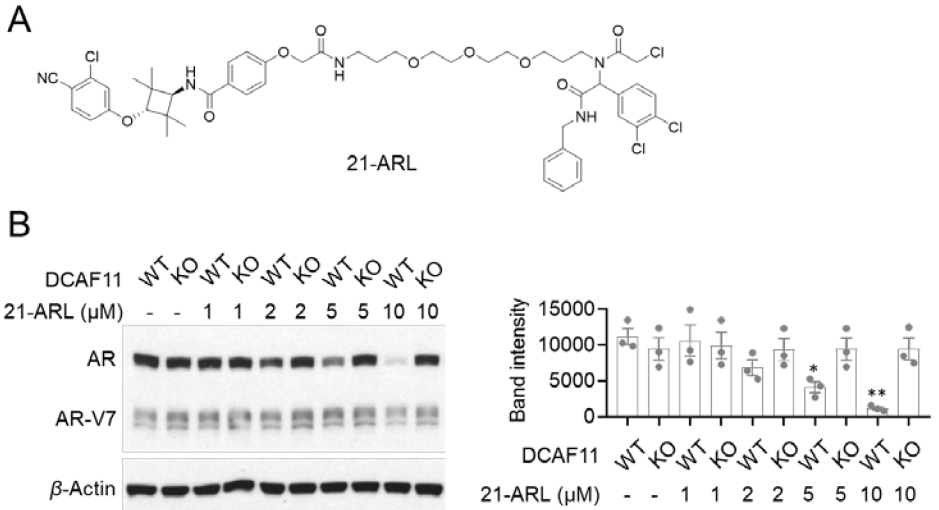

Figure 5. An electrophilic PROTAC that degrades the androgen receptor (AR) in a DCAF11-dependent manner.

A. Structure of 21-ARL, a candidate AR-directed electrophilic PROTAC. **B**. Concentration-dependent degradation of AR in DCAF11-WT and DCAF11-KO 22Rv1 cells following treatment with 21-ARL (1–10 μM) for 8 h. The result is representative of three biologically independent experiments. Bar graph (right) represents quantification of the AR content. Data are mean ± SEM (n = 3). Statistical significance was calculated with unpaired two-tailed Student's t-tests comparing 21-ARL-treated DCAF11-WT to DCAF11-KO cells at each concentration. $*P < 0.05$, $**P < 0.01$.